The computation of vector magnetic anomalies: a comparison of techniques and errors

Michael E. Purucker

ST Systems Corp., Geology and Geomagnetism Branch, Code 622, Goddard Space Flight Center, Greenbelt, MD 20771 (U.S.A.)

ABSTRACT

Purucker, M.E., 1990. The computation of vector magnetic anomalies: a comparison of techniques and errors. Phys. Earth Planet. Inter., 62: 231–245.

The greater costs and uncertainties associated with the experimental determination of vector magnetic anomalies have resulted in the development of techniques by which total field anomaly measurements can be used to calculate vector magnetic anomalies. Enhanced errors are encountered in all three of the techniques considered when calculating the eastward and downward vector magnetic anomalies in the vicinity of the geomagnetic equator. Analogous errors have been described from geomagnetic field models derived solely from total field data. The equivalent source inversion technique, although requiring the greatest computer resources, exhibits the smallest errors and is the most versatile. Errors can be minimized by: (1) using a technique such as singular value decomposition to stabilize the equivalent source solution; (2) using both total field anomaly data and suitably weighted vector anomaly data when available. The space-domain convolution and frequency-domain transformation techniques require comparable computer resources. More restrictive than the equivalent source technique, they both assume a constant geomagnetic field direction and total field anomaly data collected over a regular grid at constant altitude. These techniques are therefore most appropriate for aeromagnetic surveys covering small areas. Within this framework, the space-domain convolution is superior at most mid to high magnetic inclinations and at the magnetic equator. However, the frequency-domain transformation is superior at most other low magnetic inclinations.

1. Introduction

Geomagnetic field models derived solely from scalar data exhibit systematic errors in the computed vector components, particularly in low magnetic latitudes (Hurwitz and Knapp, 1974; Lowes, 1975; Stern and Bredekamp, 1975; Stern et al., 1980; Lowes and Martin, 1987). By analogy with the main geomagnetic field, we might expect that crustal field models derived solely from total field anomaly measurements would exhibit similar errors in the computed vector anomalies. The purpose of this paper is to compare and contrast techniques used for computing vector magnetic anomalies and crustal field models with particular attention given to the errors associated with these

techniques. These questions are addressed with computer simulations. The simulations consider magnetic data acquired at both aircraft and satellite altitude.

Vector magnetic information is particularly important in low magnetic latitudes because the signatures of the equatorial electrojet and meridional current (Maeda et al., 1982) can be identified and distinguished from crustal sources most easily using vector magnetic information.

2. Theory

While a general vector field requires three orthogonal scalars at each point in space for its

characterization, the crustal and main geomagnetic fields, in the absence of external currents, have

$$\nabla \times \mathbf{B} = 0 \tag{1}$$

It follows that $\mathbf{B}$ can be expressed as the gradient of a scalar potential A. Since a scalar potential is determined by the specification of a scalar at each point in space, a number of investigators (Lourenco and Morrison, 1973; Bhattacharyya, 1977; Galliher and Mayhew, 1982; Langel et al., 1982; Kolesova and Cherkayeva, 1986) have developed algorithms for computing vector magnetic anomalies from the total field anomaly. A brief discussion of these algorithms follows.

Lourenco and Morrison (1973) developed a frequency-domain method for computing vector magnetic anomalies from the total field anomaly. A Cartesian coordinate system is chosen such that x, y and z = north, east, and down respectively. Let the direction of the total field anomaly t be defined to be along the direction of the Earth's main geomagnetic field such that

$$\frac{\partial}{\partial t} \equiv l \frac{\partial}{\partial x} + m \frac{\partial}{\partial y} + n \frac{\partial}{\partial z} \tag{2}$$

where l, m, and n are the direction cosines of the main field. Then the anomaly in the total field (ΔT) can be expressed in terms of the magnetic potential A as

$$\Delta T(x, y, z) = -\frac{\partial A}{\partial t} \tag{3}$$

The vector magnetic anomalies $\mathbf{H}_x$, $\mathbf{H}_y$, and $\mathbf{H}_z$ can be expressed in analogous form as

$$\mathbf{H}_x = -\frac{\partial A}{\partial x}$$

$$\mathbf{H}_y = -\frac{\partial A}{\partial y}$$

$$\mathbf{H}_z = -\frac{\partial A}{\partial z} \tag{4}$$

Operating on each side of (3) with first derivatives yields

$$\frac{\partial \Delta T}{\partial x} = \frac{\partial \mathbf{H}_x}{\partial t}$$

$$\frac{\partial \Delta T}{\partial y} = \frac{\partial \mathbf{H}_y}{\partial t}$$

$$\frac{\partial \Delta T}{\partial z} = \frac{\partial \mathbf{H}_z}{\partial t} \tag{5}$$

$\mathbf{H}_x$, $\mathbf{H}_y$, $\mathbf{H}_z$ and ΔT can be expressed in terms of a finite harmonic series expansion and the resulting expansions can be introduced into (5). Evaluating the derivatives and comparing the terms on both sides of the equation yields a frequency-domain relationship between ΔT and the vector magnetic anomalies $\mathbf{H}_x$, $\mathbf{H}_y$, and $\mathbf{H}_z$. These relationships are defined by Lourenco and Morrison (1973) in their eqns. (14)–(16). A previously undescribed singularity is present in the algorithm at the geomagnetic equator where $l = 1$, $m = 0$, and $n = 0$. This algorithm assumes that the direction t is fixed. Kolesova and Cherkayeva (1986) use an iterative modification of the above technique for the case where t is variable.

Bhattacharyya (1977) utilizes a space-domain convolution in order to compute vector magnetic anomalies from the total field anomaly. He first writes A and ΔT in terms of their Fourier transforms $\Phi(u, v)$ and $G(u, v)$ where u and v are the angular frequencies along the x and y axes. He then establishes the following relationship between Φ and G:

$$\Phi(u, v) = -G(u, v)/[i(lu + mv) + ns] \tag{6}$$

where $s^2 = u^2 + v^2$.

Using (6) and the equations establishing the relationships between $\mathbf{A}$ and $\mathbf{G}$ and their Fourier transforms he writes A as a convolution integral

$$A(x, y, h) = -1/4\pi^2 \Delta T(x, y, 0) * \mathbf{I}(x, y, h) \tag{7}$$

where

$$\mathbf{I}(x, y, h)$$

$$= \int\int \frac{\exp i(ux + vy)}{i(lu + mv) + ns} \exp(-sh) \, du \, dv \tag{8}$$

Equation (8) can be rewritten as a line integral which in turn can be evaluated using Cauchy's residue theorem. The residues are evaluated separately for $n > 0$, $n = 0$, and $n < 0$. Equation (7) can then be differentiated using eqn. (4) to yield a relationship between ΔT and $\mathbf{H}_x$, $\mathbf{H}_y$, and $\mathbf{H}_z$. The vector magnetic anomalies can thus be calculated by a digital convolution of the total field anomaly with the operators defined by Bhattacharyya (1977) in his eqns. (23)–(30). Unlike the

frequency-domain method, this technique has no known singularities.

Galliher and Mayhew (1982) and Langel et al. (1982) used the equivalent source technique (Dampney, 1969; Ku, 1977; Mayhew, 1979; Langel et al., 1984) in order to calculate, in a least-squares sense, the magnetic moments of a grid of equivalent source dipoles. The dipoles are calculated as follows:

$$\mathbf{p} = (\mathbf{V}\mathbf{D}^{-1}\mathbf{V}')\mathbf{S}'\mathbf{b} \tag{9}$$

where

$\mathbf{p}$ = vector whose elements are the magnetic moments of the dipoles,

$\mathbf{S}$ = matrix of the geometric source function relating the jth source to the ith position,

$\mathbf{V}$ = matrix whose elements are eigenvectors of $\mathbf{S}'\mathbf{S}$,

$\mathbf{D}$ = matrix whose diagonal contains the eigenvalues of $\mathbf{S}'\mathbf{S}$,

$\mathbf{b}$ = vector of observations.

The matrix $\mathbf{D}$ is modified using singular value decomposition so that small eigenvalues and their inverses are set to 0. E_p, the percentage of the trace of $\mathbf{D}$ that is retained, is selected so as to reduce the standard deviation to typical mid-latitude values. An E_p of between 95 and 99% is found to satisfy this requirement. An E_p of the 97% is used in this analysis unless otherwise indicated.

The elements of the geometric source function matrix $\mathbf{S}$ are:

$$\mathbf{S}_{ij} = \frac{\partial \mathbf{F}_i}{\partial \mathbf{p}_j} \tag{10}$$

These $\mathbf{S}_{ij}$ relate the $\mathbf{F} = (\Delta T, \mathbf{H}_x, \mathbf{H}_y, \mathbf{H}_z)$ magnetic field at $i(r, \theta, \phi)$ to the magnitude of the dipole source $(\mathbf{p})$ at $j(r', \theta', \phi')$

Total field or vector magnetic anomalies can then be calculated from these dipoles. This algorithm will work with either fixed or variable t and can be used with ungridded measurements taken at multiple elevations above the magnetic source. Because of these advantages, it has been the method of choice for satellite magnetic surveys. The equivalent source method, however, requires greater computer resources than either the frequency-domain transformation or the space-domain convolution method.

3. Computer simulations

The computer simulations reported here use two exact and one approximate forward modelling schemes in order to calculate the total field and vector magnetic anomalies expected at an array of observation points over a magnetic source. The grid of total field anomaly data is then used to calculate vector magnetic anomalies on that same grid and compared with the exact or approximate forward modelling results.

The exact forward modelling algorithms used here have been developed for use with rectangular (Bhattacharyya, 1964) and polygonal (Plouff, 1976) prisms. They are developed in rectangular coordinates and hence assume a 'flat-earth' geometry.

An approximate spherical-earth algorithm (Ku, 1977; Von Frese et al., 1980) developed for use with MAGSAT data, was also used for forward modelling. The technique utilizes Gauss–Legendre quadrature integration and linear interpolation between adjacent boundary points in order to calculate equivalent source dipoles given source volume shapes and magnetizations. The magnetic field calculated from each equivalent source dipole is then summed at the observation point. For effective resolution, the distance from the magnetic body to the observation point must be greater than the distance between nodes or dipoles (Ku, 1977). In the case discussed here the observation plane is 430 km above the Earth's surface whereas the equivalent source dipoles are 8–55 km apart.

3.1. Frequency-domain transformation

The accuracy of the frequency-domain transformation can be evaluated by comparing the vector magnetic anomalies computed using this transformation to the values calculated employing an exact forward modelling scheme (Plouff, 1976). The vector magnetic anomalies are calculated as follows: The total field anomaly is first transformed using a two-dimensional discrete Fourier transform (FFT) with an array size of 64 × 64. This size was chosen in order to minimize edge effects and to produce smooth contours. Array sizes as large as 90 × 90 and as small as 8 × 8 produce qualitatively similar results. The discrete

DELTA T   H$_x$ FREQUENCY DOMAIN   H$_x$

TRANSFORMATION

DECL =   5.0

INCL =   2.0

CONTOUR INTERVAL: 1 UNIT

H$_Y$ H$_z$ H$_Y$ H$_z$

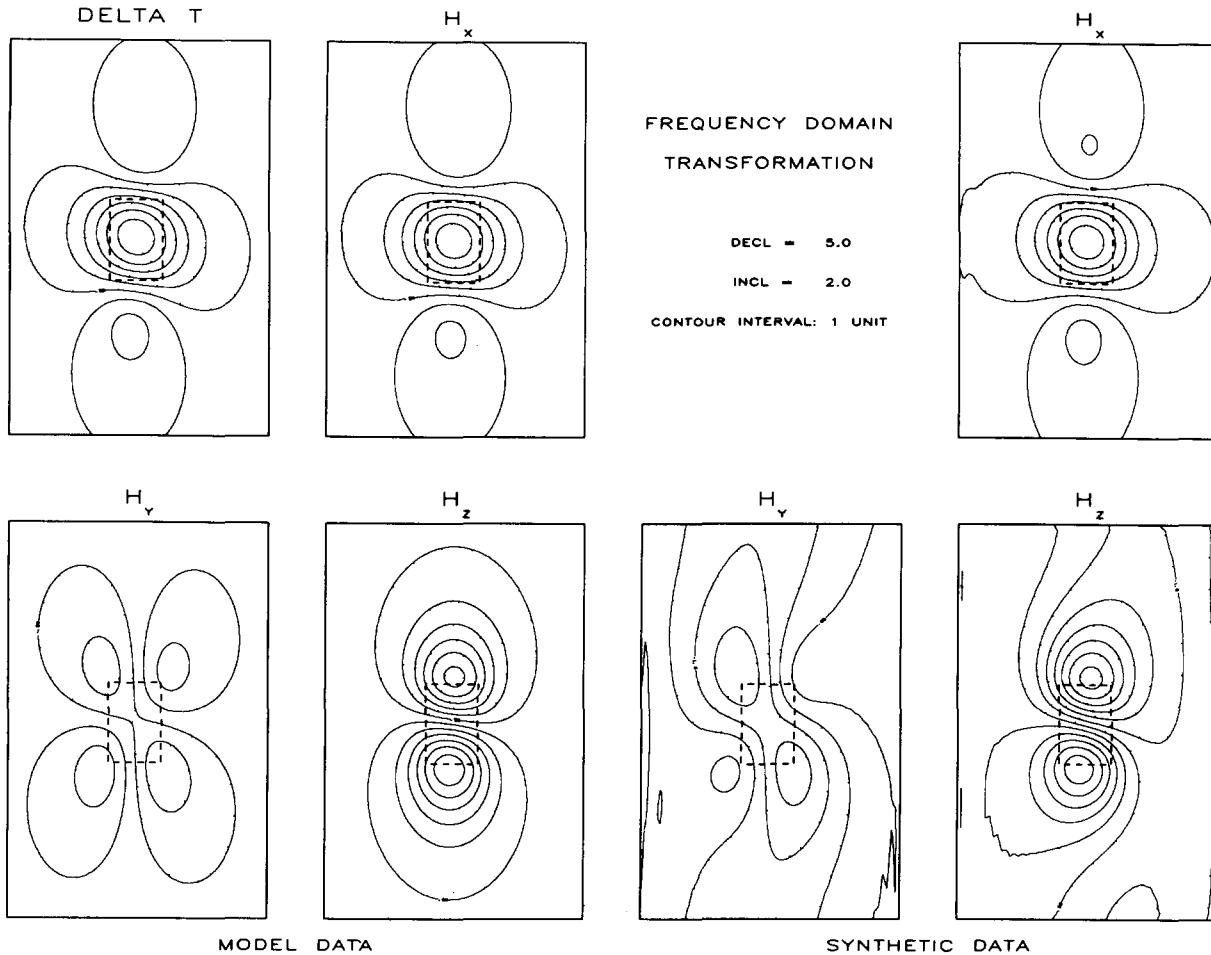MODEL DATA   SYNTHETIC DATA

Fig. 1. Comparison of 'model' and 'synthetic' magnetic field data calculated using a frequency-domain transformation. The magnetic source is outlined by dashed lines. Negative values are indicated with hash marks. 'Model' data, shown on the left, are calculated using an exact algorithm (Plouff, 1976) developed for use on a 'flat earth'. Frequency-domain transformations are then applied to the total field anomaly in order to compute the corresponding vector magnetic anomalies. These latter anomalies are termed 'synthetic' fields and are shown on the right.

The simple magnetic source is a prism with horizontal dimensions of 12.8 × 12.8 units and a vertical depth of 10 units. The magnetic source is centred on a 64 × 64 grid and the transformation is done using that same grid. The magnetic source is magnetized by induction. All magnetic fields are calculated at a distance of 6.4 units above the source.

Fourier transform is then multiplied by an operator and finally back-transformed to the space domain. A depth-limited magnetic source located in the centre of the array ensures that the mean value of the field is effectively 0. This mean value is evaluated using eqns. (18)–(20) of Lourenco and Morrison (1973).

Vector and total field anomalies calculated using an exact forward modelling scheme are referred to as 'model data' (Fig. 1). The vector field

anomalies calculated using the frequency-domain transformation of the total field anomaly are referred to as 'synthetic data' (Fig. 1).

The differences between the model and synthetic data sets can be quantified and expressed as a percentage error (P_e), where

$$P_e = \frac{\sum \sum |F_m - F_s|}{\sum \sum |F_m|} \times 100 \qquad (11)$$

% ERROR IN FREQUENCY

DOMAIN TRANSFORMATION AS A

FUNCTION OF INCLINATION

AND DECLINATION

CONTOUR INTERVAL: 10%

STIPPLING INDICATES WHERE
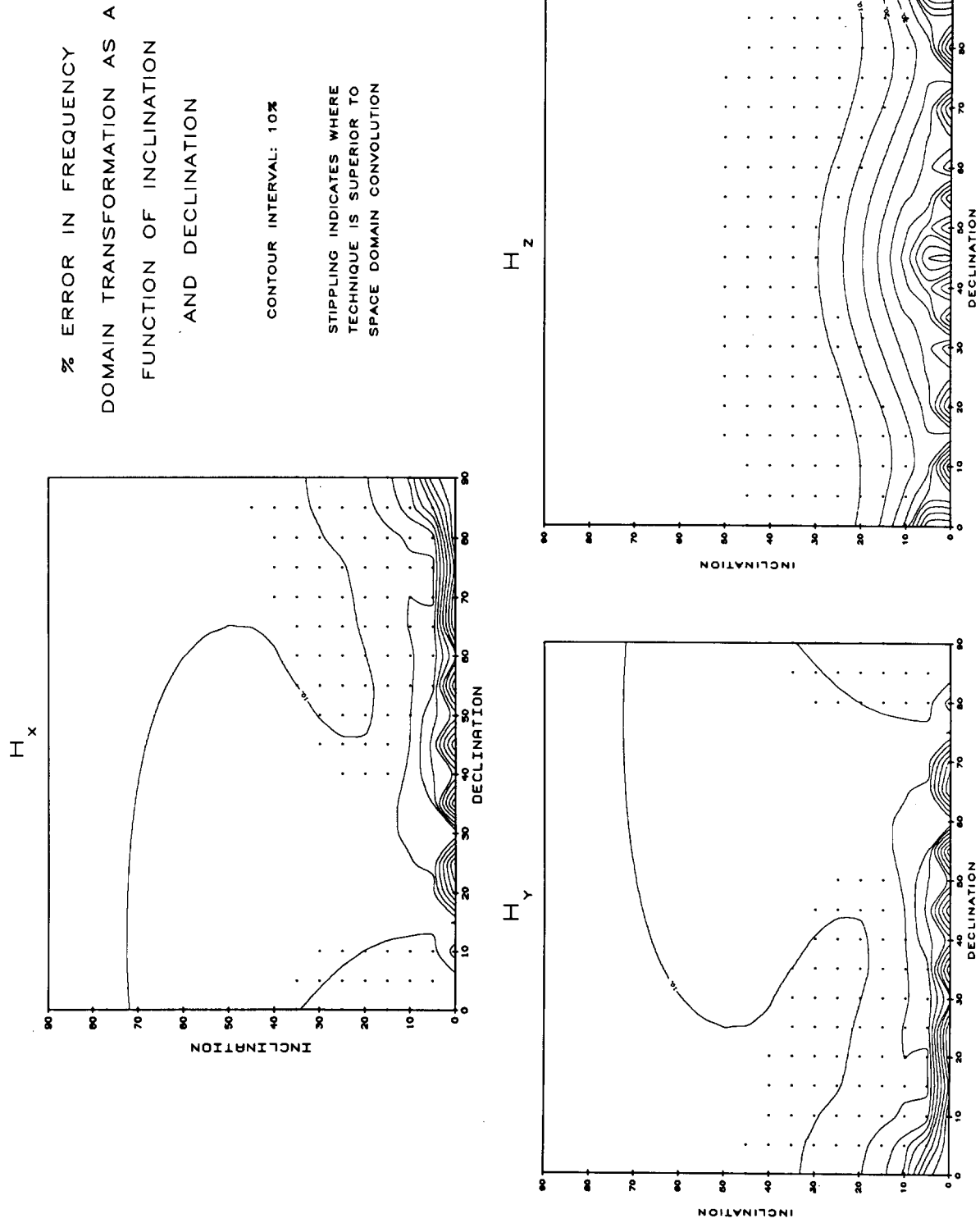TECHNIQUE IS SUPERIOR TO
SPACE DOMAIN CONVOLUTION

Fig. 2. Contours of the percentage error, a quantification of the differences between 'model' and 'synthetic' data, as a function of magnetic declination and inclination. The 'model' and 'synthetic' data are calculated as in Fig. 1. The percentage error is calculated using eqn. (11) in the text. Edge effects are minimized by stripping off the 10 outermost rows and columns from the matrix before computing the percentage error. The percentage error is evaluated on 5 degree intervals in declination and inclination.

DELTA T   H$_x$ H$_x$

SPACE DOMAIN

CONVOLUTION

DECL — 5.0

INCL — 2.0

CONTOUR INTERVAL: 1 UNIT

H$_y$ H$_z$ H$_y$ H$_z$
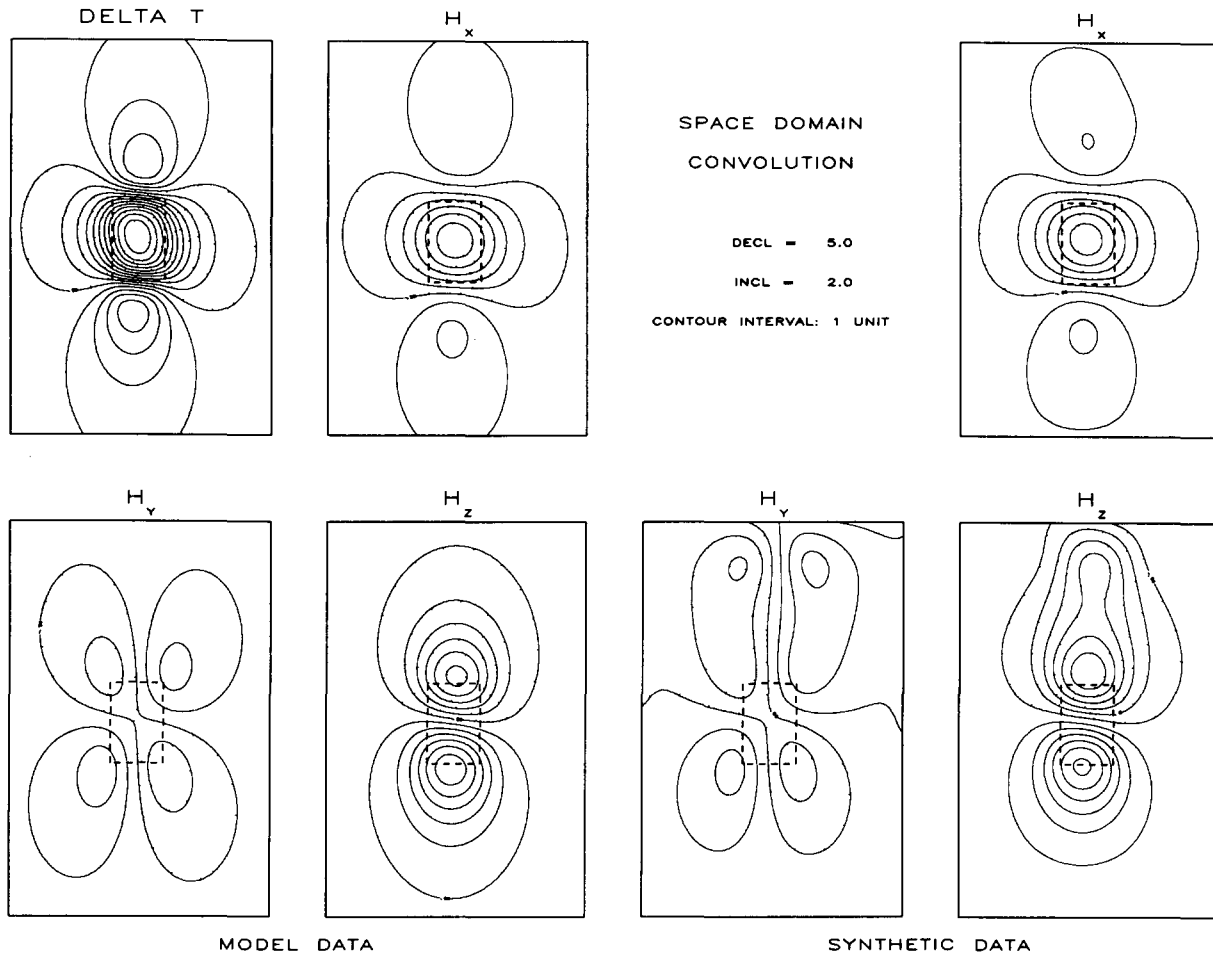
MODEL DATA   SYNTHETIC DATA

Fig. 3. Comparison of 'model' and 'synthetic' magnetic field data calculated using a space-domain convolution. The space-domain convolution is applied to the total field anomaly in order to compute the corresponding vector magnetic anomalies. The space-domain convolution is calculated using a 64×64 window.

The total field anomaly is calculated at a distance of 3.4 units above the source. The vector magnetic anomalies are calculated at a distance of 6.4 units above the source. Other information is as given in Fig. 1.

where
F_m = the 'model data' and
F_s = the 'synthetic data'.

The sums are taken over that portion of the data set which is not contaminated by edge effects.

The results, presented in Figs. 1 and 2, indicate a maximum percentage error in excess of 90% for the H_y and H_z components near the magnetic equator. The closest correspondence between the model and synthetic data sets occurs at mid to high inclinations. The poorest correspondence oc-

curs in low-inclinations, particularly in the H_y and H_z components.

3.2. Space-domain convolution

The accuracy of the space-domain convolution can be evaluated by comparing the vector magnetic anomalies computed using this approach to the values calculated using an exact forward modelling scheme (Plouff, 1976). The vector magnetic anomalies are calculated as follows. A space-domain convolution is applied to the total field

% ERROR IN SPACE DOMAIN
CONVOLUTION AS A FUNCTION
OF INCLINATION AND
DECLINATION

CONTOUR INTERVAL: 10%

STIPPLING INDICATES WHERE
TECHNIQUE IS SUPERIOR TO
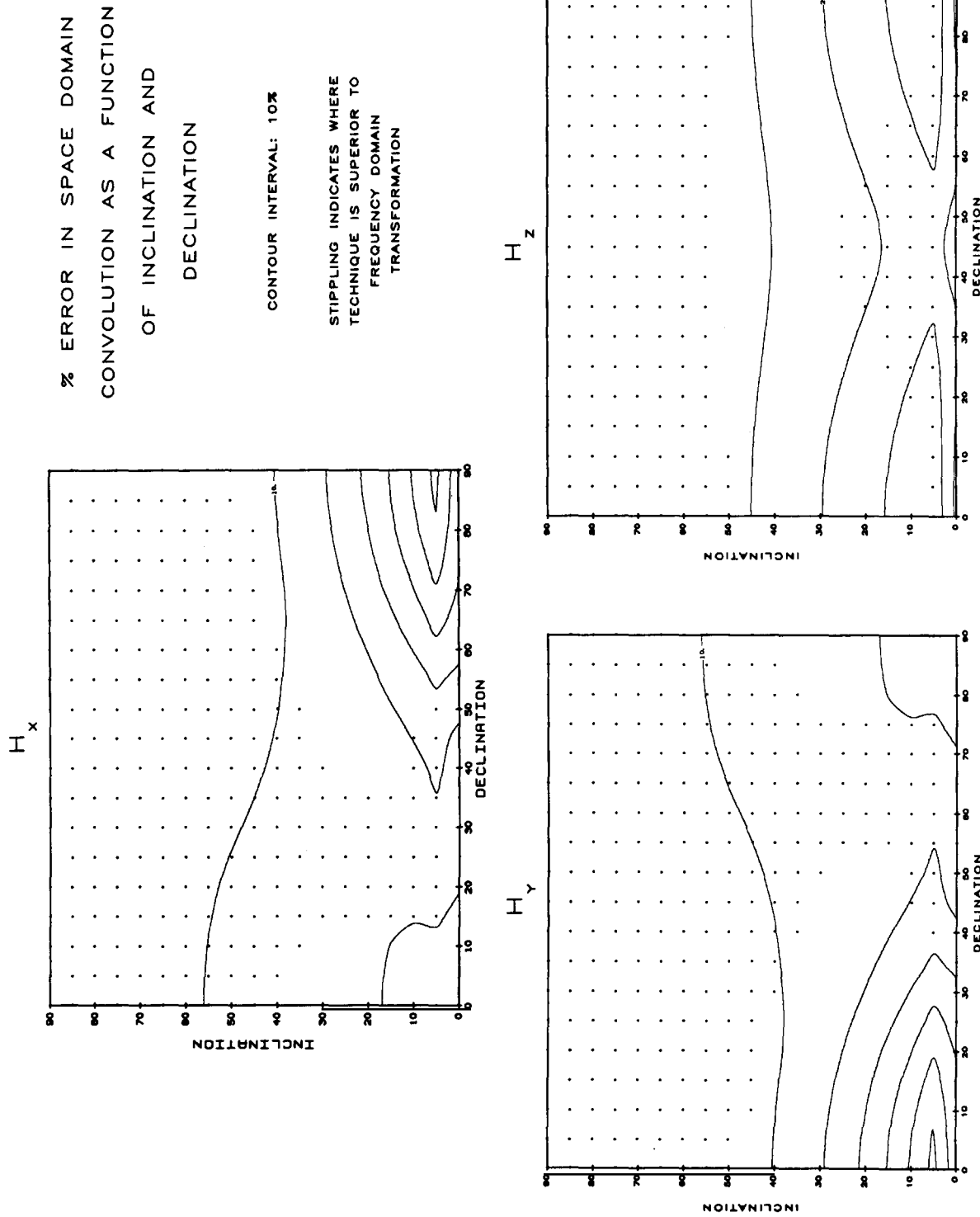FREQUENCY DOMAIN
TRANSFORMATION

Fig. 4. Contours of the percentage error as a function of magnetic declination and inclination. The 'model' and 'synthetic' data are calculated as in Fig. 3 except that the space-domain convolution is calculated using a 21×21 window. Edge effects are minimized by stripping off the three outermost rows and columns from the matrix before computing the percentage error. Other information is as given in Fig. 2.

anomaly using a window of (64 × 64). This size was chosen in order to compare the results with that of the frequency domain transformation. Array sizes as small as 21 × 21 produce qualitatively similar results.

The results (Figs. 3 and 4), presented in a way analogous to the frequency-domain transformation, indicate a maximum percentage error in excess of 60% in the H_y component near 5° inclination. The closest correspondence between the model and synthetic data sets occurs at mid to high inclinations. The poorest correspondence occurs in low inclinations, particularly in the H_y and H_z components. The improvement of the space-domain convolution between 5° inclination and the magnetic equator is a consequence of using different convolution operators for the two cases. If the convolution operator used for $n > 0$ had been used at the magnetic equator, the percentage errors on H_y and H_z would have doubled.

Bhattacharyya (1977) illustrated his technique with an example which crosses the geomagnetic equator. Errors of the type discussed in this paper can probably be seen in the H_y vector anomaly at the geomagnetic equator (fig. 9 of Bhattacharyya, 1977) but are not apparent in H_z (fig. 10 of Bhattacharyya, 1977) although they may be masked by the lack of significant anomalies near the geomagnetic equator. Bhattacharyya claims that his approach is superior to the frequency-domain transformation in low latitudes around the geomagnetic equator. As shown in Figs. 2 and 4, if the percentage error is used to evaluate and compare the two techniques, the space-domain convolution is superior at most mid to high magnetic inclinations and at the magnetic equator. However, the frequency-domain transformation is superior at most other low magnetic inclinations. Improvements could be made in the space-domain convolution technique by evaluating equation (8) to higher order using Cauchy's residue theorem. As noted earlier, when this is done at the geomagnetic equator, the percentage error decreased by a factor of 2 for H_y and H_z.

3.3. Equivalent source inversion

Equivalent source inversion uses a least-squares algorithm (Mayhew et al., 1984), in conjunction with singular value decomposition (Langel et al., 1984) in order to estimate the values of magnetic moments located on a grid at the Earth's surface from a much larger set of ungridded magnetic field values collected at multiple altitudes. These dipoles can then be used to calculate the expected magnetic field at any altitude.

The dipoles in the equivalent source representation are assumed to carry a magnetization only in the direction of the ambient field. The inversion produces both positive and negative values. As discussed by Harrison et al. (1986), only positive values should result from induction, which is assumed to be the primary source of magnetization. The presence of both positive and negative values illustrates that the zero level is non-unique. Since the dipoles are only an intermediate step and not a final product, we have not applied an annihilator (e.g. Parker and Huestis, 1974) to produce exclusively positive values.

The grid of equivalent source dipoles used in the inversion extends over the entire map. The dipoles are not confined to the region of the magnetic body but include a larger region, encompassing the entire region shown on Fig. 5. Restricting the dipoles to the magnetic body implies an a-priori knowledge of the location of the magnetic body. In the general case, the location of the magnetic body is unknown.

The resolution of the equivalent source technique is such that the distance between the observation plane and the equivalent source dipoles must be larger than the distance between individual equivalent source dipoles (Ku, 1977). In our case the observation plane is 430 km above the Earth's surface whereas the equivalent source dipoles are 110 km apart and are located within the upper 40 km of the Earth's crust.

Singular value decomposition is used to stabilize the equivalent source solution. Instability is particularly acute in the vicinity of the magnetic equator, where a straight inversion produces 'ringing' in the resultant dipoles, with large negative and positive values alternating.

Vector and total field anomalies calculated at satellite altitude using the approximate spherical-earth algorithm are referred to as 'model data'. These fields are shown in the upper two rows of
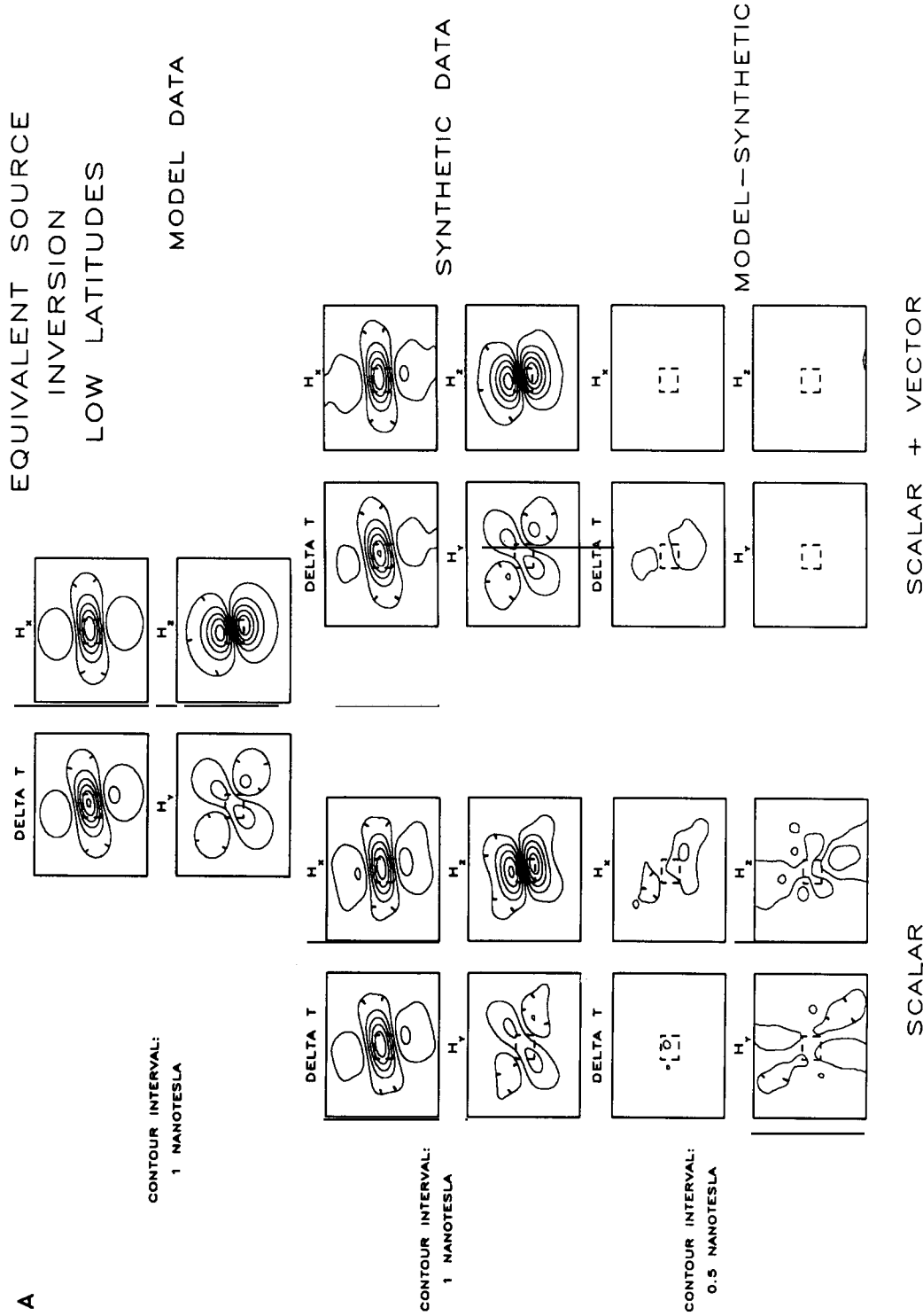
Fig. 5A, B. Comparison of 'model' and 'synthetic' magnetic field data calculated using an equivalent source inversion. Grid size is 50 × 50.

The simple magnetic source is a prism 440 km on a side and extending from the surface to a depth of 33 km. The magnetic fields associated with this source are evaluated with equivalent source dipoles. The dipoles are spaced at 55-km intervals horizontally and 16-km intervals vertically. The magnetic source has a susceptibility contrast of 0.05 SI. The magnetic source is magnetized by induction. The field is calculated at an altitude of 430 km.

The dipoles from which the 'synthetic' data are calculated are located within regions 1° (110 km) on a side at the equator. These dipoles cover the entire map, not just the magnetic source.

A field model of degree and order 13 (Langel and Estes, 1985) is used as the inducing field and provides the inclination and declination of the main field.

A. The low-latitude case has a field inclination of 2° and a declination of −14° at the centre of the grid. The magnetic source lies at the centre of a square grid which extends from 27.5° west to 2.5° west and from 3.5° south to 21.5° north.

B. The mid-latitude case has a field inclination of 39° and a declination of −10° at the centre of the grid. The magnetic source lies at the centre of a square grid which extends from 25° west to the central meridian and from 15° north to 40° north.

EQUIVALENT SOURCE
INVERSION
MID LATITUDES

MODEL DATA

SYNTHETIC DATA

MODEL–SYNTHETIC

SCALAR + VECTOR

SCALAR

CONTOUR INTERVAL:
1 NANOTESLA

CONTOUR INTERVAL:
1 NANOTESLA

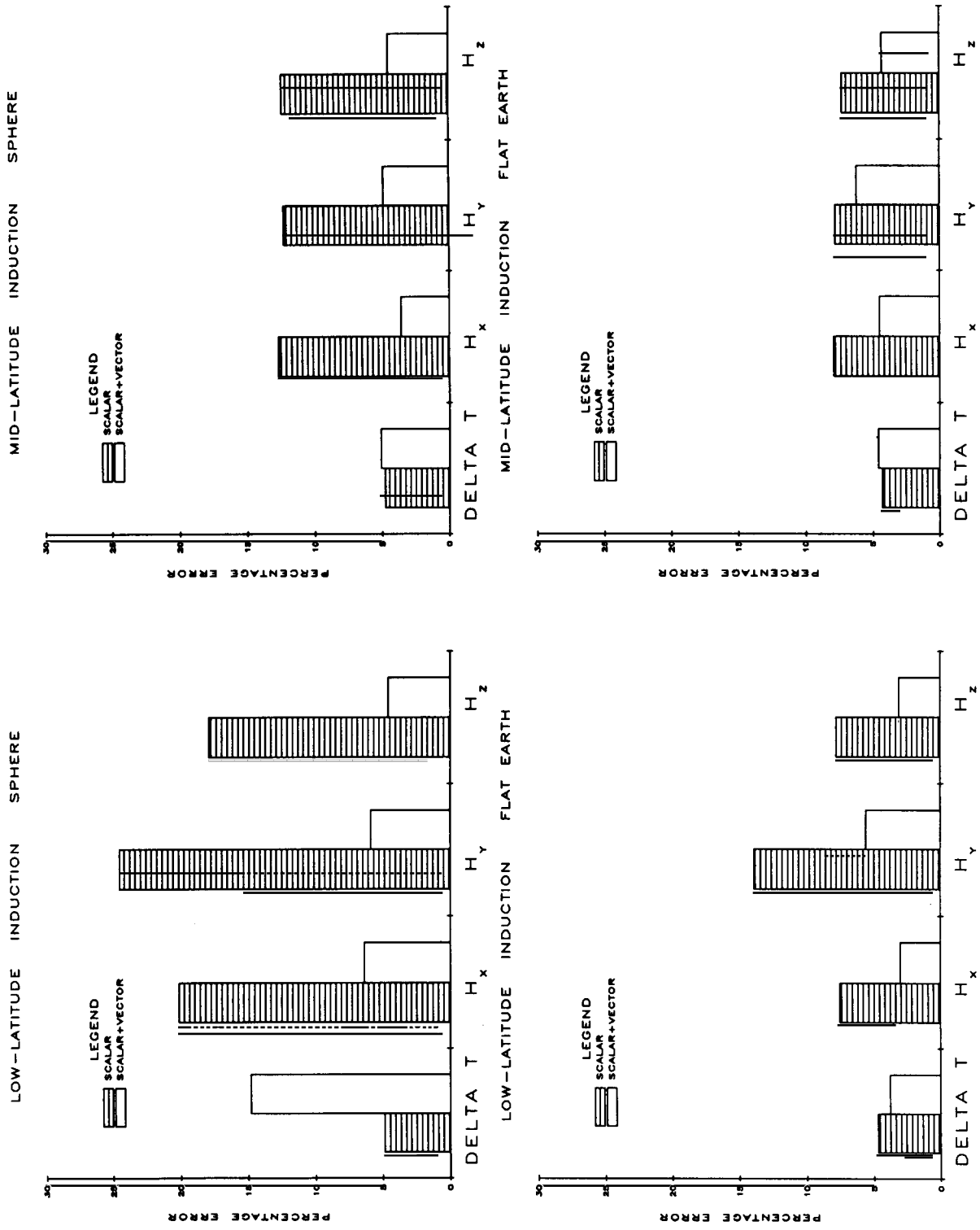CONTOUR INTERVAL:
0.5 NANOTESLA

B

Fig. 6. Histograms depicting the percentage error of the equivalent source solutions. The histograms series in the upper left corner corresponds to the 'model' and 'synthetic' data shown in Fig. 5A. The histogram series in the upper right corner corresponds to the data shown in Fig. 5B. The histogram series in the lower left and right corners were calculated using the 'flat earth' forward algorithms of Bhattacharyya (1964) and are more approriate for magnetic data collected from aircraft altitude.
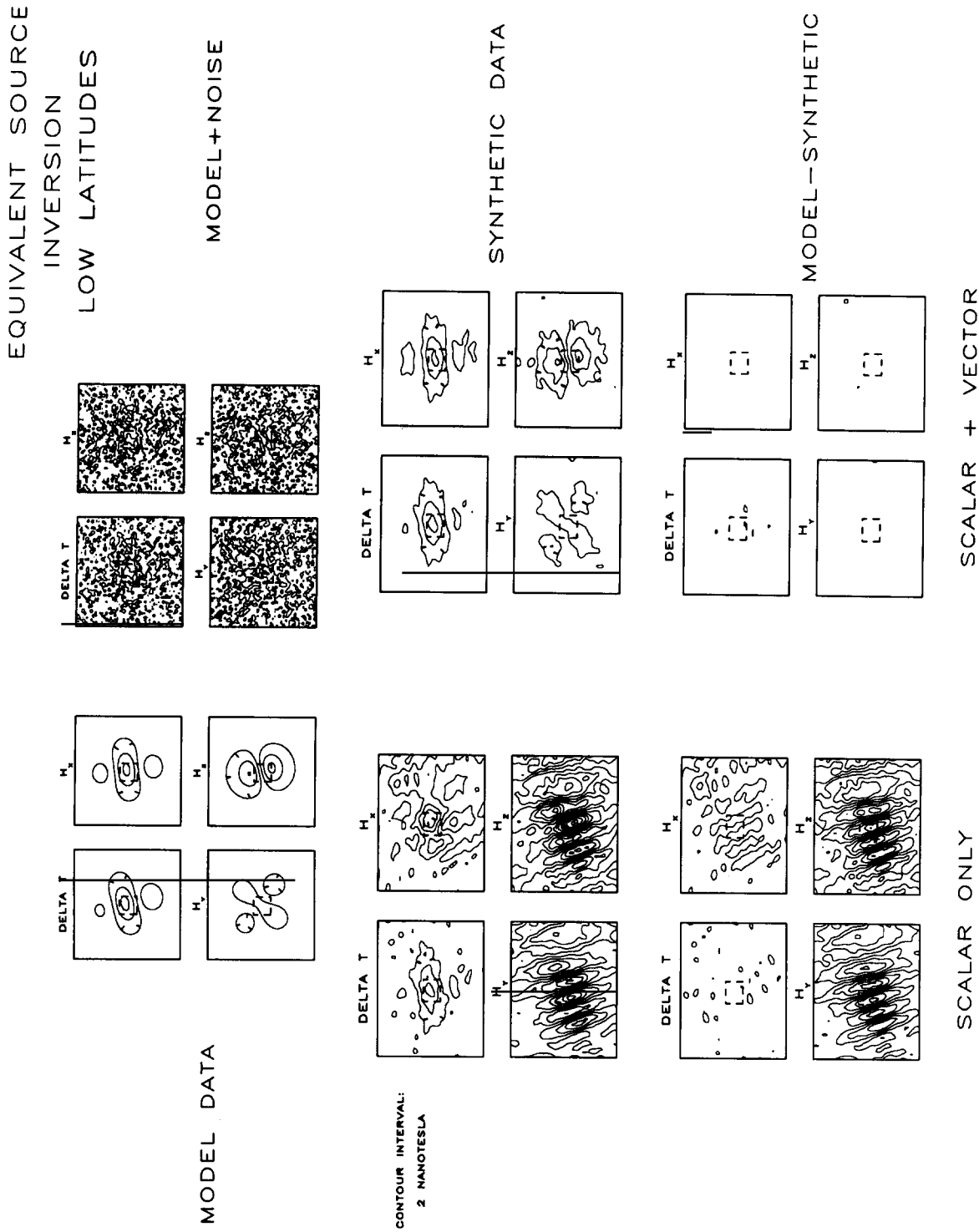
Fig. 7. Comparison of 'model' and 'synthetic' magnetic field data calculated using an equivalent source inversion with added random noise. The magnetic source is located astride the magnetic equator. The equivalent source inversion is performed with minimal singular value decomposition (E_p = 99.99999%). 'Model' data, shown in the upper left corner, are calculated using a forward algorithm developed for the spherical earth. The pseudo-random noise, shown along with the model data in the upper right corner, has an approximate r.m.s. of 1 nT and zero mean. All other parameters are identical to those in Fig. 5A.

Fig. 5A, B. The 'model data' are then inverted to an equivalent source distribution which in turn is used to calculate the vector and total field anomalies at satellite altitude again. These latter fields are referred to as 'synthetic data' and are shown in the middle two rows of Fig. 5A, B. These 'synthetic' fields are calculated using total field anomaly data alone, shown in the left two columns of Fig. 5A, B, and using vector and total field anomaly data, shown in the two righthand columns of Fig. 5A, B. The difference between the 'model data' and the 'synthetic data' is then calculated and is shown in the lower two rows of Fig. 5A, B. These experiments are performed for both low-latitude (Fig. 5A) and mid-latitude (Fig. 5B) magnetic distributions. The illustrated results are for sources magnetized by induction.

The results indicate a maximum percentage error of 25% in the H_y component near the geomagnetic equator. The closest correspondence between the model and synthetic data sets occurs in mid-latitudes (Fig. 5B) where both vector and total field anomaly data are used in the inversion. The poorest correspondence between the model and synthetic data sets occurs in low latitudes (Fig. 5A) where total field anomaly data alone are used in the inversion.

Histograms of the percentage errors are shown in Fig. 6. These histograms illustrate that while mid-latitude models are recovered more accurately than low-latitude models, the presence or absence of vector anomaly data in the inversion is the primary factor in determining how well the model will be recovered.

If the observation plane is changed from satellite altitude (430 km) to aircraft altitude (1 km) we may use the exact algorithms of Bhattacharyya (1964), developed for use on a 'flat earth'. A closer correspondence exists between the model and synthetic data (Fig. 6) when the data are acquired at aircraft altitude. The 'aircraft' data are also noteworthy because of the absence of any degradation in the total field anomaly data set at low latitudes when the synthetic total field anomaly data are reconstructed from the model total field and vector anomaly data.

Normally distributed pseudo-random noise was added to the model data in order to simulate experimental data (Fig. 7). The noise has an approximate r.m.s. of 1 nT and zero mean. This noise level is comparable to that encountered in the MAGSAT data (Langel et al., 1982). For comparison, the absolute maximum of the total field anomaly model is 6 nT. The model data with added noise are then inverted to an equivalent source distribution as above. For the induction case using total field anomaly data alone at low magnetic latitudes, the results indicate that the nearly orthogonal H_y and H_z vector components are not recovered at all in the presence of noise with minimal ($E_p = 99.99999$) singular value decomposition applied to the least-squares solution. The 'ringing' or 'bulls-eye' pattern present in the field value solutions is analogous to the pattern present in the underlying dipole solutions. Singular value decompositions using an E_p of less than 99.9% are necessary before this feature is removed from the solutions.

4. Discussion

Enhanced errors are encountered in all three of the discussed techniques when calculating the eastward and downward anomalies in the vicinity of the geomagnetic equator. Analogous errors have been described from geomagnetic field models derived solely from total field data. The errors in the geomagnetic field models have been related by some to the proof of Backus (1970), that the scalar potential A is not uniquely determined by the measurement of the magnitude of the total field outside the magnetic source.

The equivalent source inversion technique, although requiring the greatest computer resources, generates the smallest errors and is the most versatile. Errors can be minimized by using a technique such as singular value decomposition to stabilize the equivalent source solution. At low latitudes in the presence of noise, vector components oblique to the total field anomaly are not recovered at all from the total field anomaly data alone if singular value decomposition is not used. An E_p of 99.9% or less will allow first-order recovery of the vector components and will also suppress 'ringing' or 'bulls-eye' patterns in the

vector solutions. Errors can also be minimized by using both total field anomaly data and suitably weighted vector anomaly data when available. Because vector data are noisier than total field anomaly data for a given uncertainty in altitude, it may be necessary to use different weights for the different data types. When we invert observational data using the equivalent source technique, we assign to each observation a weight which corresponds to the standard error of all observations of its type (i.e. total field or vector) in the immediate vicinity. The dipoles are then calculated as follows:

$$p = (VD^{-1}V')S'Wb \qquad (12)$$

where:

V = matrix whose elements are eigenvectors of S'WS,

D = matrix whose diagonal contains the eigenvalues of S'WS,

W= diagonal weight matrix.

and with other symbols as defined in (9). The addition of weights to the problem has the further advantage that errors can then be calculated on the dipoles, and by propagation, on the field values.

The space-domain convolution and frequency-domain transformation techniques require comparable computer resources. More restrictive than the equivalent source technique, they both assume a constant geomagnetic field direction and total field anomaly data collected over a regular grid at constant altitude. These techniques are therefore most appropriate for aeromagnetic surveys covering small areas. Within this framework, the space-domain convolution is superior at most mid to high magnetic inclinations and at the magnetic equator. However, the frequency-domain transformation is superior at most other low magnetic inclinations.

Acknowledgments

References

Backus, G.E., 1970. Non-uniqueness of the external geomagnetic field determined by surface intensity measurements. J. Geophys. Res., 75: 6339–6341.

Bhattacharyya, B.K., 1964. Magnetic anomalies due to prism-shaped bodies with arbitrary polarization. Geophysics, 29: 517–531.

Bhattacharyya, B.K., 1977. Reduction and treatment of magnetic anomalies of crustal origin in satellite data. J. Geophys. Res., 82: 3379–3390.

Dampney, C.N.G., 1969. The equivalent source technique. Geophysics, 45: 39–53.

Galliher, S.C. and Mayhew, M.A., 1982. On the possibility of detecting large-scale crustal remanent magnetization with MAGSAT vector magnetic anomaly data. Geophys. Res. Lett., 9: 325–328.

Harrison, C.G.A., Carle, H.M. and Hayling, K.L., 1986. Interpretation of satellite elevation magnetic anomalies. J. Geophys. Res., 91: 3633–3650.

Hurwitz, L. and Knapp, D.G., 1974. Inherent vector discrepancies in geomagnetic main field models based on scalar F.J. Geophys. Res., 79: 3009–3013.

Kolesova, V.I. and Cherkayeva, Ye.A., 1986. Computation of the components of the anomalous magnetic field from the data of absolute surveys for a variable direction of the vector of the main field. Geomagn. Aeron., 26: 884–885.

Ku, C.C., 1977. A direct computation of gravity and magnetic anomalies caused by 2- and 3-dimensional bodies of arbitrary shape and arbitrary magnetic polarization by equivalent-point method and a simplified cubic spline. Geophysics, 42: 610–622.

Langel, R.A. and Estes, R.H., 1985. The near-earth magnetic field at 1980 determined from MAGSAT data. J. Geophys. Res., 90: 2495–2509.

Langel, R.A., Slud, E.V. and Smith, P.J., 1984. Reduction of satellite magnetic anomaly data. J. Geophys., 54: 207–212.

Langel, R.A., Schnetzler, C.C., Phillips, J.D. and Horner, R.J., 1982. Initial vector magnetic anomaly map from MAGSAT. Geophys. Res. Lett., 9: 273–276.

Lourenco, J.S. and Morrison, H.F., 1973. Vector magnetic anomalies derived from measurements of a single component of the field. Geophysics, 38: 359–368.

Lowes, F.J., 1975. Vector errors in spherical harmonic analysis of scalar data. Geophys. J. R. Astron. Soc., 42: 637–651.

Lowes, F.J. and Martin, J.E., 1987. Optimum use of satellite intensity and vector data in modelling the main geomagnetic field. Phys. Earth Planet. Inter., 48: 183–192.

Maeda, H., Iyemori, T., Araki, T. and Kamei, T., 1982. New evidence of a meridional current system in the equatorial ionosphere. Geophys. Res. Lett., 9: 337–340.

Mayhew, M.A., 1979. Inversion of satellite magnetic anomaly data. J. Geophys., 45: 119–128.

Mayhew, M.A., Estes, R.H. and Myers, D.M., 1984. Remanent magnetization and three-dimensional density model of the Kentucky anomaly region. Final report of NASA contract NAS5-27488, 90 pp.

Parker, R.L. and Huestis, S.P., 1974. The inversion of magnetic anomalies in the presence of topography. J. Geophys. Res., 79: 1587–1593.

Plouff, D., 1976. Gravity and magnetic fields of polygonal prisms and application to magnetic terrain corrections. Geophysics, 41: 727–741.

Stern, D.P. and Bredekamp, J.H., 1975. Error enhancement in geomagnetic models derived from scalar data. J. Geophys. Res., 80: 1776–1782.

Stern, D.P., Langel, R.A. and Mead, G.D., 1980. Backus effect observed by MAGSAT. Geophys. Res. Lett., 7: 941–944.

Von Frese, R.B., Hinze, W.J., Braile, L.W. and Luca, A.J., 1980. Spherical earth gravity and magnetic anomaly modeling by Gauss-Legendre quadrature integration. Final report of NASA Contract NAS5-25030, 116 pp.